Investigating metal-inhibitor interaction with EQCM and SVET: 3-amino-1,2,4-triazole on Au, Cu and Au-Cu galvanic coupling

J. A. Ramírez-Cano, L. Veleva, R.M. Souto and B. M. Fernández-Pérez

1. Introduction

Copper and its alloys are present in almost every aspect of modern life; they are employed extensively in industry ranging from building components to microelectronic applications [1]. Copper is a relatively resilient metal to corrosion in neutral environments and in the absence of chlorides and SO_2, protected by the formation of a corrosion product (Cu_2O), known as patina. However, it is susceptible to corrosion in aggressive media, when the patina is converted to other corrosion products [2].

There are several methods to prevent the metallic corrosion and one of them is the use of inhibitors (either organic or inorganic). Organic inhibitors are compounds that applied in very small concentrations are capable of effectively reduce the corrosion rate [3]. Among these compounds those belonging to the group of azoles, which contain nitrogen and/or sulphur, are considered to be effective corrosion inhibitors for copper in a wide range of aggressive environments [4-8].

Inhibitor selection is often based on the gravimetric determination of metal dissolution rate (i.e., mass loss). However, this method provides very little information about the complex interactions between the metal, the inhibitor and the corrosive media. So, in order to optimize inhibition, the involved mechanism in such interactions must be known. This demands the use of electrochemical techniques and surface analysis in the corrosion laboratory. Most of the actual knowledge of the inhibition process of corrosion has been obtained through the use of conventional electrochemical methods such as cyclic voltammetry, chronoamperometry, and electrochemical impedance spectroscopy (EIS) [9].

The development of *in-situ* scanning probe techniques has allowed the surface characterization with micrometric scale resolution or even smaller. The combination of

spatial resolution and chemical sensibility is of great use in this field to determine the operation variables and the reaction mechanisms. The systems that can be studied with these scanning microelectrochemical techniques (namely, the scanning vibrating electrode-technique (SVET) [10], scanning electrochemical microscopy (SECM), scanning electrochemical impedance microscopy (SEIM), scanning ion-conductance microscopy (SICM), and localized electrochemical impedance spectroscopy (LEIS) include the protection characteristics of polymeric films applied on metals and their underfilm degradation [10-12], the preferential dissolution of one metal in alloys and galvanic pairs [13], the formation thin protective films by adsorption of organic inhibitory molecules over passive metal films [14, 15], tip modification for reactive metal sensing [16, 17] and fabrication of robust ion selective micro-electrodes for potentiometric analysis [18].

The high local resolution of such techniques (SVET, SECM, LEIS and AC-SECM) combined with the possibility of probe operation in an electrochemical cell, allows direct characterization of the involved electrochemical processes of the corrosion phenomena. An electrochemical activity mapping (current density, pH, etc…) of the surface of interest in contact with the electrolyte can be performed in-situ and in real time, as well as surface modification (mainly, pitting initiation at specific places, localized surface scaling, adsorbed film degradation, etc…).

The electrochemical quartz crystal microbalance (EQCM) is another valuable electrochemical technique that allows the acquisition of relevant data about the adsorption of molecules on metallic surfaces within the micro-scale resolution enabling the characterization of their adsorption kinetics. [3, 19-23]. The technique works by applying an oscillatory electrical field to a quartz resonator placed between two electrodes made of the metal of interest, this makes the resonator to vibrate at its fundamental frequency. The frequency is sensible to the mass of the resonator and when adsorption or desorption occurs on the metallic surfaces it is detected as a frequency shift.

In this work, the scanning vibrating electrode technique (SVET) and the quartz crystal microbalance technique (EQCM) were used to characterize the electrochemical interaction

of two corrosion inhibitors, 2-Mercaptobenzothiazole and 3-Amino-1,2,4-triazole (ATA), in Au and Cu samples individually and with both metals connected in order to form a galvanic pair Au-Cu.

2. Experimental Part

2.1. Materials

Reactive grade inhibitors were employed, acquired from Aldrich, with a purity of 97% for 2MBT and of 95% for ATA. Aqueous solutions were prepared using bi-distilled water (18.2 MΩ cm) with concentrations ranging from 100 to 1mMwith a step of 1 order of magnitude. For EQCM measurements the whole range of concentrations was used and for SVET all experiments were performed at 1 mM concentration.

In the case of the EQCM experiments the working electrodes are made of AT-cut quartz crystals with a fundamental frequency of 10 MHz where the metal of interest is electrodeposited in both faces of the crystal. The electrodes have an electroactive area of 0.205 cm^2 and are manufactured by GAMRY Instruments. The essays were carried out in a GAMRY Teflon cell, specifically designed to be used with the EQCM electrodes unique shape.

For SVET measurements Pt/Ir (80%/20%) probes of 2-3 cm in length were used, coated by parelene C except at the tip, so that only this end works as sensor, were used. Additionally, two reference Pt electrodes are used; these Pt electrodes must be coated by black platinum. The probes must be platinized with the purpose of creating a spherical black platinum deposit of 10-20 µm of diameter. All experiments were carried out in constant height mode, with the tip initially at 100 µm from the surface and a peak to peak amplitude of 100 µm.

Mapped samples in SVET were manufactured employing Au and Cu wires of electrolytic grade (99.999%) with diameters of 500 and 125µm respectively, and embedding them in Epofix resin (Struers, Ballerup, Denmark) in this way samples of Au, Cu and the galvanic couple Au-Cu were prepared.

2.2. OCP measurements

The open circuit potential (Free Corrosion Potential, OCP) measurements were carried out on the manufactured samples by creating a small container using adhesive tape and the treatment solution 1mM 2MBT, ATA or NaCl was added to the container.

The OCP of Au, Cu and the galvanic pair Au-Cu were recorded during 60 minutes on an AUTOLAB (Metrohm, Herisau, Switzerland) bipotentiostat, controlled by a personal computer. The reported values correspond to the mean value and it was corrected taking into account the potential of the Ag/AgCl/KCl (3M) reference electrode.

2.3. EQCM measurements

The observed frequency shifts due to inhibitor adsorption were measured in-situ, adding the inhibitor solution directly to the Teflon cell. Once the frequency shifts are recorded, they are fitted to the Langmuir kinetic model (Eq. 1 and 2) [3, 21] to obtain the adsorption parameters such as the adsorption constant (k_a), the desorption constant (k_d), the equilibrium constant ($K_{eq}=(k_a)(k_d)^{-1}$) and finally the adsorption free energy (ΔG_{ads}) (Eq. 3).

$$\theta(t-t_0)=K'[1-e^{(km)(t-t0)}] \quad (1)$$

$$K'=C[C+(kd)(ka^{-1})]^{-1} \quad (2)$$

$$\Delta G_{ads}=-RTlnK_{eq} \quad (3)$$

In equation 1(θ) represents the coated area; (t)is time; (t_0) is the diffusion time and (k_m) is the obstruction constant, which is related to the adsorption and desorption constants by equation 4.

$$k_m=k_aC+k_d \quad (4)$$

In equation 3(R) is the universal gas constant and (T) is temperature.

2.4. SVET scans

The samples studied in SVET were submerged for 60 minutes in the inhibitor solution, then rinsed, using ethanol and finally taken to the SVET where the essay solution 1mM NaCl is added. The scanned area is defined by hand, so it's almost impossible to obtain the same area for each scan. However, the scanned area for each sample is always very similar and the area difference between scans can be neglected. The mapping lasts one hour, for a total of 10 scans, one each 6 minutes. In this way the spatial distribution of the current density is obtained and is possible to distinguish between anodic or cathodic behavior in the sample. The results are graphically presented using an algorithm programmed in MATLAB that allows the acquisition of isometric and/or XY plane graphics.

3. Results and Discussion

3.1. OCP analysis

The mean OCP values recorded for each system are shown in Table 1.

Table1

OCP Average [mV]

Sample	1mM NaCl	1mM ATA	1mM 2MBT
Au-Cu	-437.2	-428.2	-459.6
Au	-149.5	-115.8	-207.2
Cu	-286.4	-296.9	-417.4

From the values reported in Table 1, we can see that ATA has a slight inhibitive effect on Au and the Au-Cu pair, ΔOCP=33.7 mV and ΔOCP=9 mV respectively. However, in the case of Cu there is no protection effect at all on the contrary it makes the OCP slightly more negative ΔOCP =-10.5 mV and thus facilitates the corrosion process, an interesting fact having in to account that ATA is considered to be a good Cu corrosion inhibitor [22-25].

On the other hand, 2MBT makes the OCP of all samples (Au, Cu and Au-Cu) more negative reducing the Au-Cu pair OCP by ΔOCP=-22.4 mV, the Au OCP by ΔOCP=-57.7 mV and the Cu

OCP by ΔOCP=-131 mV. It's quite interesting to see that the bigger change in OCP has taken place in copper, given that 2MBT is considered to be a good corrosion inhibitor for copper [2, 3, 5-7], we should expect to see a shift toward more positive OCP values in Cu exposed to 2MBT.

3.2. EQCM measurements of inhibitor adsorption: change of frequency vs time

3.2.1. Au in ATA aqueous solutions

The frequency shift for the adsorption of ATA on Au is presented in figs. 1 (the fitted curve is in red). The curves are obtained inverting the Y axis ($-\Delta f$ vs t). The observed frequency shifts follow a well-defined exponential behavior, ruled by the Langmuir kinetic model of an adsorption process. The fit parameters for the Langmuir kinetic model are shown in table 2 as a function of ATA concentration. It can be seen that the experimental data are in very good agreement (R^2) with the fitted model.

Table 2

Langmuir fit parameters as a function of ATA concentration for the system ATA-Au

ATA [mM]	R^2	K'	k_m[s^{-1}]	t_0[s]
100	0.98	0.98	$1.93x10^{-3}$	26.95
10	0.99	7.82	$1.15x10^{-3}$	18.46
1	0.99	28.75	$1.61x10^{-3}$	-29.77

The adsorption (k_a=5.4×10^{-3} M^{-1} s^{-1}) and desorption (k_d=1.4×10^{-3} s^{-1}) constants were obtained from equation 3, and using these values the equilibrium constant (K_{eq}=3.85) was got. The

free energy of adsorption (ΔG_{ads}) was calculated (-3.29 kJ mol^{-1}), using equation 2; this value corresponds to a physisorption process [3, 26, 27].

It is reported that in aqueous solution, ATA stablishes a tautomeric equilibrium, which gives place to an anionic form of ATA [28]. This anionic form is able to react/adsorb through its terminal nitrogen [28, 29]. In this way, it will create a physical barrier between the environment and Au surface.

On the other hand, the presence of the ATA molecules on gold probably reduces the amount of adsorbed water molecules on Au, maintaining the energy excess on gold surface. This suggestion could explain the measured more noble OCP value on Au in ATA solutions (table 1).

3.2.2. Cu in ATA aqueous solutions

The frequency shifts for the adsorption of ATA on Cu are presented in figs. 2(the fitted curve is in red) and they present an exponential behavior, according to the Langmuir kinetic model. The correlation coefficients and the adsorption fit parameters are shown in table 3. Following the same procedure employed in the ATA-Au system, were obtain the adsorption

Table 3

Langmuir fit parameters as a function of ATA concentration for the system ATA-Cu

ATA [mM]	R^2	K'	k_m[s^{-1}]	t_0[s]
100	0.99	459.82	$1.28x10^{-3}$	29.58
10	0.99	478.75	$2.12x10^{-3}$	50.15
1	0.99	138.87	$1.31x10^{-3}$	-10.84

(k_a=-4×10^{-3} M^{-1} s^{-1}) and desorption (k_d=1.7×10^{-3} s^{-1}) constants, the equilibrium constant (K_{eq}=2.35) and the calculated adsorption free energy (ΔG_{ads}=-2.12 kJ mol^{-1}), corresponding to a spontaneous physisorption process.

By comparing the calculated adsorption free energy (ΔG_{ads}) values obtained for each system, ATA-Au (Table 2) and ATA-Cu (Table 3), it could be considered that ATA is physisorbed in both metals, with energy values that lie beneath the theoretical chemisorption threshold [3]. In this case of ATA the involved heteroatom is nitrogen, which acts as an anchorage point between both metals (Cu and Au) and the anionic form of ATA. However, it is not capable of forming a strong bond with the metal surface.

On the other hand, the frequency shift difference between both metals (figs.1 and 2) is very high, having a maximum Δf of 22.5 Hz for 1mM ATA on gold, while the same concentration for Cu yields a Δf of 330 Hz. The higher frequency shift observed on copper (one order of magnitude) could be attributed to the initial stages of corrosion on copper surface given that the OCP value (Table 1) turns to a more negative value (ΔOCP=181.1 mV) compared to Au. It could be concluded that ATA has a negative effect on Cu, instead of protecting it. We assume that the ATA film acts as some kind of electron transfer mediator between Cu and the solution.

Azoles have been studied employing several techniques, which confirm that these compounds have a high affinity for noble metals, because of the highly electronegative heteroatoms (S, N, O, etc…) present in their structure [6, 30, 31]

3.2.3. Au and Cu in 2MBT aqueous solutions

The results concerning the adsorption of 2MBT on Au and Cu had been published elsewhere [3, 27]. The obtained adsorption energies correspond to spontaneous physisorption processes with reported values of -8.11 kJ mol^{-1} and -5.59 kJ mol^{-1}, respectively. In those works, was proposed that the adsorption of 2MBToccurs through the terminal exo-sulphur of the anionic form of 2MBT, which is exposed once the tautomeric equilibrium is established. It is well known that sulphur presents a high affinity for gold [32-34] and this is

why the energy adsorption of 2MBT on gold (-8.11 kJ mol^{-1}) is higher than on copper (-5.59 kJ mol^{-1}).

The measured OCP of Au, Cu and Au-Cu (table 1), revealed that in the presence of the inhibitor 2MBT there is a shift to more negative values than those recorded in NaCl solution. The most significant change is observed on copper having his average OCP displaced by 131 mV.

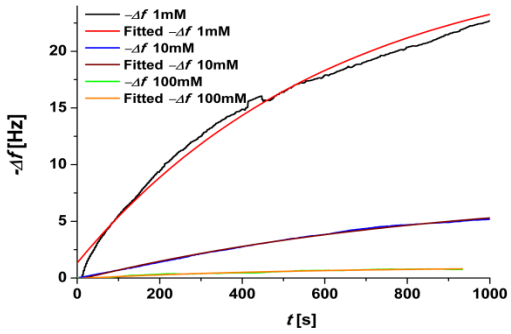

Figure 1. Frequency shift for the adsorption of ATA on Au from 1mM, 10mM and 100mM aqueous solution

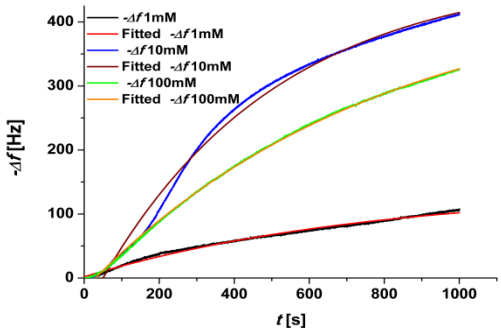

Figure 2. Frequency shift for the adsorption of ATA on Cu from 1mM, 10mM and 100mM aqueous solution

3.3. SVET surface analysis

All SVET maps are carried out using the manufactured Au and Cu electrodes, described in the experimental part, with 500 µm and 125 µm of diameter respectively, in the case of the pair the separation between both metals is approximately 1.8 mm.

3.3.1. Current density maps in absence of corrosion inhibitors

3.3.1.1. Au sample

a) b)

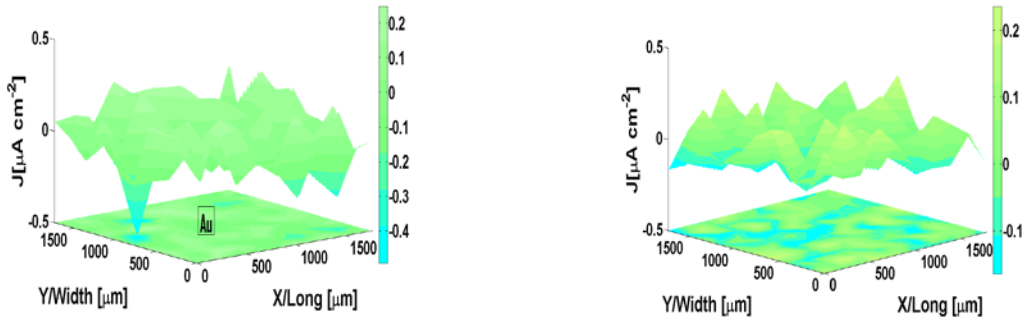

c)

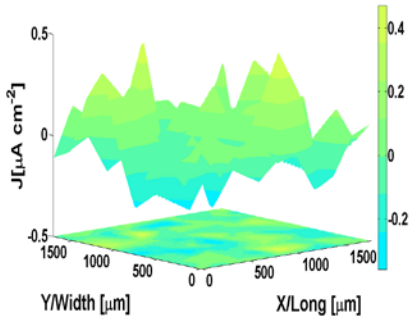

Figure 3. Current density maps for Au in 1mM NaCl at 6 min (a), 30 min (b) and 60 min (c).

Figure 3, presents the current density maps for naked Au in 1 mM NaCl, we can see that gold surface can't be resolved which can be explained by low reactivity of gold in NaCl solution. The current density range remains very stable during the scan of the sample, oscillating between -0.5 and 0.5 µA cm^{-2}.

3.3.1.2. Cu sample

a) b)

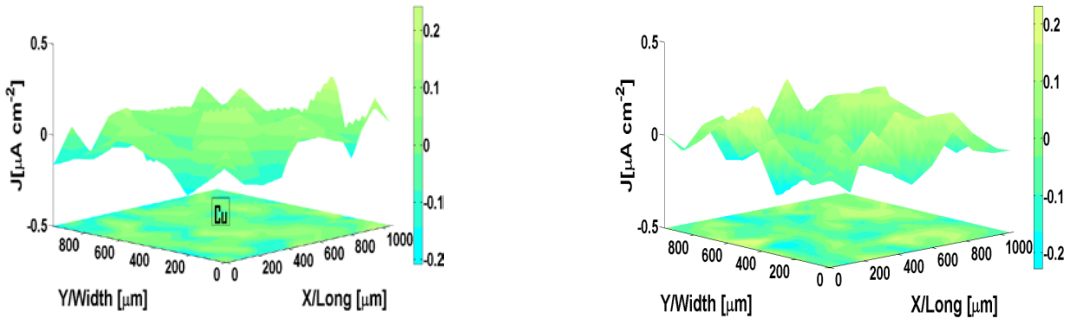

c)

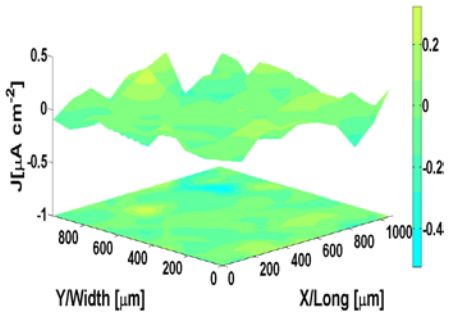

Figure 4. Current density maps for Cu in 1mM NaCl at 6 min (a), 30 min (b) and 60 min (c).

The current density maps of naked copper are presented in figure 4, the scan shows very low electrochemical activity in 1 mM NaCl with his current density range oscillating between -0.5 and 0.3 µA cm^{-2}. The low activity could be due to the passivation of copper, leaving ionic flux in solution as the only source of electrochemical activity.

3.3.1.3. Au-Cu sample

a)

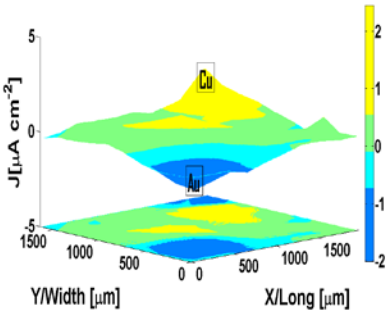

b)

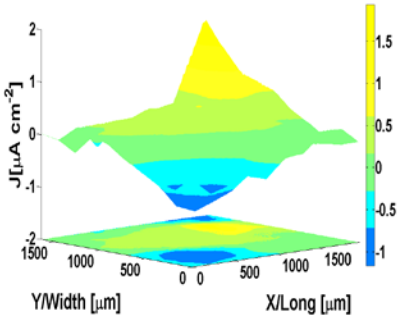

c)

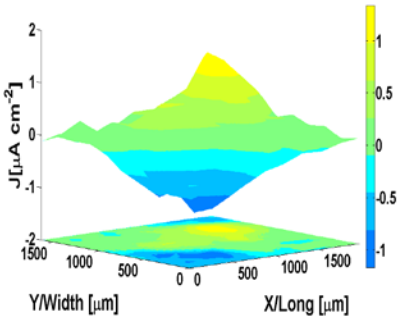

Figure 5. Current density maps for Au-Cu pair in 1mM NaCl at 6 min (a), 30 min (b) and 60 min (c).

Figure 5 presents the scans of the Au-Cu pair in 1mM NaCl, in this case it is possible to resolve both metals, which is to be expected since the electrical coupling between both metals forces the anodic behavior on copper and the cathodic behavior on gold. Current density range remains fairly stable with a maximum range oscillating between -2 and 2 µA cm^{-2}.

3.3.2. Current density maps in presence of corrosion inhibitors

3.3.2.1. Au sample treated with ATA

a) b)

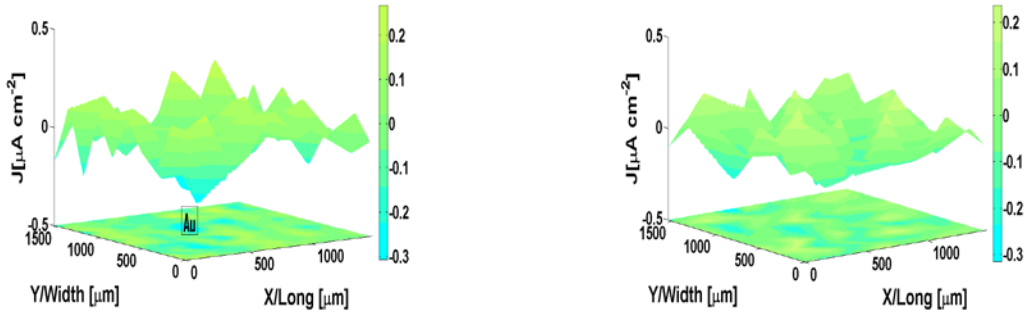

c)

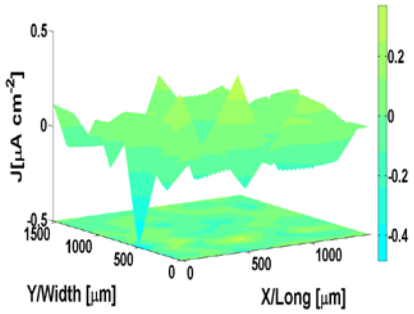

Figure 6. Current density maps for Au treated with 1 mM ATA in 1 mM NaCl at 6 min (a), 30 min (b) and 60 min (c).

Figure 6 presents the current density maps of Au treated with ATA 1mM for 60 minutes, if we compare these results to the current density maps of Figure 7, we can see that the behavior of both systems is very similar, gold surface can't be resolved in presence or absence of ATA and the current density range is practically the same. The detected electrochemical activity is almost certainly due to ionic flux in the bulk of the solution.

If we look at the OCP values for each system in table 1, we can see that the difference between them is only 33.7 mV and therefore we can expect a very similar electrochemical behavior. The fact that the presence of ATA on gold turns the OCP to more positive values,

will lead us to believe that he electrochemical activity on treated Au will be lower than the one found in non-treated gold, if we put our attention towards the current density range, on each system, we can see that it there is practically no difference between treated and non-treated gold.

Furthermore, the EQCM measurements show that the frequency variation of ATA adsorbing on Au is very low, 22.5 Hz (Fig. 1), implying that only a small number of ATA molecules are present during the SVET scan, since this kind of inhibitor operates forming a physical barrier between the electrolyte and the aggressive environment any possible contribution by ATA to the protection of gold will be very small.

3.3.2.2. Au sample treated with 2MBT

a) b)

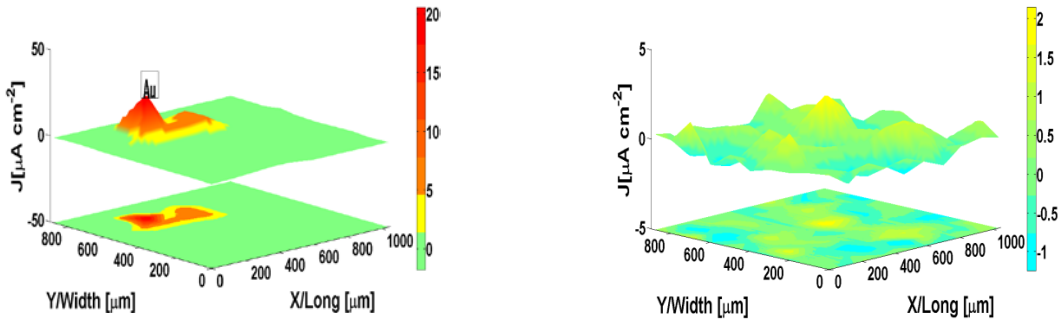

c)

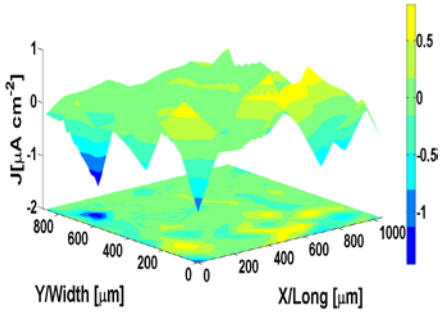

Figure 7. Current density maps for Au treated with 1 mM 2MBT in 1 mM NaCl at 6 min (a), 30 min (b) and 60 min (c).

The current density maps of the Au-2MBT system are presented in Figure 7. Contrary to what was observed in previous cases (Figs. 4 and 6), it is possible to resolve gold's surface in the first 6 minutes of the scan, Fig. 7a shows clearly a high anodic activity localized on Au surface. Also, the current density range is considerably higher when compared to all previous cases (Figs. 4, 5 and 6) going from -1.75 to 20 μA cm^{-2}. From the current density range we can see that, at the beginning of the scan (6 minutes, fig. 7a), the main contribution is of anodic nature could be attributed to the tautomeric equilibrium of 2MBT, which implies the deprotonation of the molecule [35], this stage of the tautomeric equilibrium is what SVET is detecting as anodic activity.

Given that ATA is also a tautomer, we might wonder why we don't see the same effect on gold (Fig. 6). And the answer could be that when ATA adsorbs on Au surface it forms a monolayer film, while 2MBT forms a multilayer film which will be less stable and more prone to molecular detachment. Since the calculated free adsorption energy of ATA on Au (-3.29 kJ mol^{-1}) is lower than the adsorption energy of 2MBT on Au (-8.11 kJ mol^{-1}) we can expect to have more 2MBT molecules than ATA molecules, a fact that is supported by the EQCM frequency variation measurements which show that the frequency variation of ATA adsorbing on gold is much lower than the one observed in 2MBT adsorption on gold [27].These additional 2MBT molecules could detach from the multilayer film and, once in aqueous solution, resume their tautomeric equilibrium deprotonating and appearing in the SVET scan as anodic activity. So, as these detached molecules spread in the bulk of the solution we lose the initial surface resolution, because there is no more localized-deprotonation on top of Au surface. As a result of this homogenization of electrochemical activity, the current density range decreases although it maintains a wider range than the one observed in naked and ATA treated Au.

The OCP values for this system (Table 1) also indicate that 2MBT has a negative effect, pushing the OCP to more negative values. However, this result could not be due to an accelerated corrosion process, but the tautomeric equilibrium described above. In this way, 2MBT will act as a multi-mechanism inhibitor, forming a multilayer physical barrier and also

interacting with the electrolyte by detaching the outermost molecules and probably forming compounds with the electroactive species present in solution.

3.3.2.3. Cu sample treated with ATA

a) b)

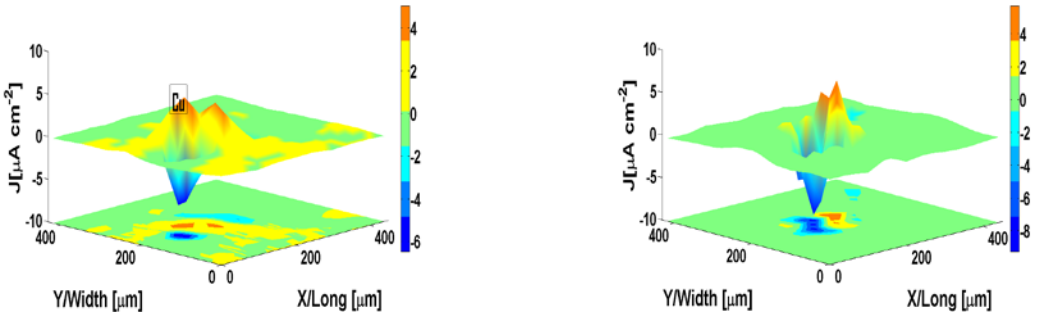

c)

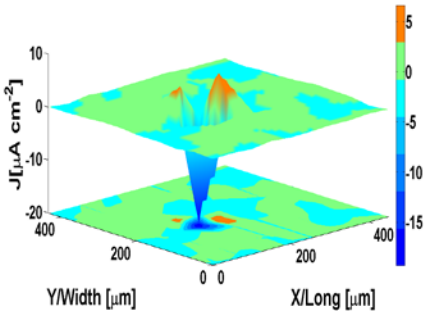

Figure 8. Current density maps for Cu treated with 1 mM ATA in 1 mM NaCl at 6 min (a), 30 min (b) and 60 min (c).

Figure 8, presents the current density distribution on the copper sample treated with 1mM ATA. It can be seen that there are very well defined anodic and cathodic areas on Cu surface and the current density range is one order of magnitude higher than the one found on naked Cu (Fig. 4). The presence of ATA increases considerably the electrochemical activity, enabling the resolution of copper surface and increasing the current density range to a maximum of -20 to 7 µA cm^{-2}.

From the OCP measurements (Table 1), we can see that the ATA treatment makes the OCP more negative by 10.5 mV, as discussed before, this effect could be due to ATA working as

an electron transfer mediator between the metallic surface and the solution or because of chemical interaction between ATA and Cu, given that ATA adsorption energy on copper falls beneath the chemisorption threshold, and thus is unable to chemically interact with Cu, we suppose that ATA works as an electron transfer facilitator once adsorbed on Cu.

Also, the EQCM measurements show a higher frequency shift for ATA on Cu (Fig. 2) than for ATA on Au (Fig. 1), the adsorption of ATA on gold has a maximum frequency variation of 22.5 Hz for 1mM ATA while the same concentration on Cu has a Δf of 330 Hz. This implies that the amount of adsorbed mass on Cu is also one order of magnitude higher than the mass adsorbed on Au, under this scenario it is very possible that ATA is able to form a monolayer over Cu that will facilitate electron migration from the metal to the solution. Given that the monolayer, ideally, covers the entire copper surface the presence of ATA will enable SVET to resolve Cu surface with high detail.

3.3.2.4. Cu sample treated with 2MBT

a)

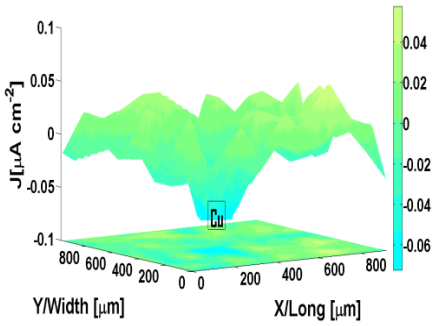

b)

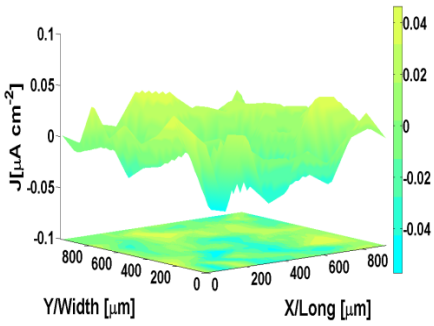

c)

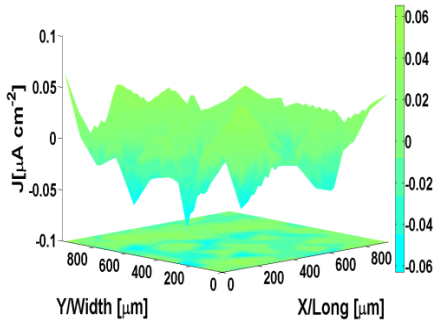

Figure 9. Current density maps for Cu treated with 1 mM 2MBT in 1 mM NaCl at 6 min (a), 30 min (b) and 60 min (c).

The Cu-2MBT system is presented in figure 9, as we can see the Cu surface treated with 2MBT is visible in the first 6 minutes of the scan but eventually disappears, considering that the electrode diameter is of 125 µm and that the electrochemical activity observed after 6 minutes is outside the area of the electrode, at 30 minutes. The ability to resolve Cu surface could be due to the presence of adsorbed 2MBT on Cu that is electrochemically interacting with the electrolyte.

It is worth noticing, that the current density range for the treated sample is considerably lower than the one found in the non-treated sample since after 30 minutes falls within the base cero color used in the color map. At this point, the current density range is one order of magnitude lower and remains, basically, the same for the rest of the scan.

This result supports the idea that the OCP displacement to more negative values only corresponds to the protonation/deprotonation process that takes place in the tautomeric equilibrium of 2MBT in aqueous solution and not the metal being attacked by the inhibitor.

The adsorption energy and frequency variation of 2MBT on Cu [3] is lower than 2MBT on Au [27], this differs significantly from what was observed with ATA on Cu and Au but is expected since thiazole compounds have higher affinity for gold than azole compounds. Therefore, 2MBT molecules will find more suitable active sites on gold than on copper giving place to a thicker film. The higher adsorption energy also adds stability to the film, favoring the formation of a multilayer structure on gold that can survive the ethanol rinsing previous to SVET measurement, while copper may not be capable to provide a god substrate for the formation of a multilayer 2MBT film.

In this way there will be less 2MBT molecules capable of resuming their tautomeric equilibrium once in aqueous NaCl solution and therefore we can’t see the anodic activity present in 2MBT treated Au. Also, the OCP value of the 2MBT-Cu system is considerably more negative than the NaCl-Cu and 2MBT-Au systems, this could be due to the presence of a higher number of 2MBT molecules present in the bulk of the solution, given that Cu is not capable of adsorb as many molecules as gold can, in this way the amount of molecules

protonating and deprotonating in the 2MBT-Cu system is considerably higher and gets translated as a more negative OCP value.

3.3.2.5. Au-Cu sample treated with ATA

a) b)

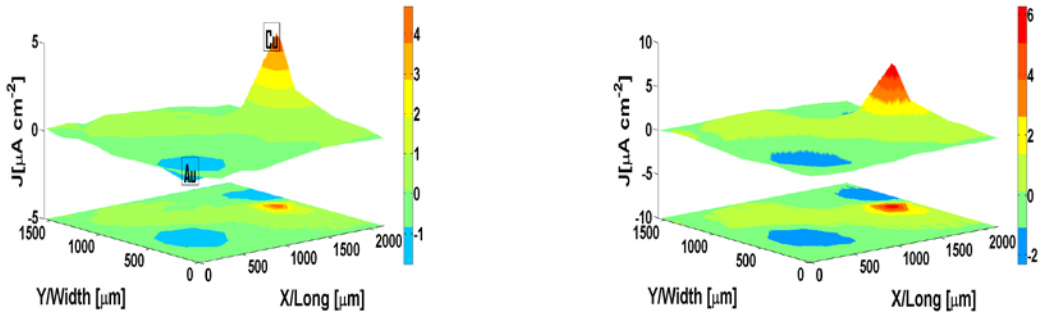

c)

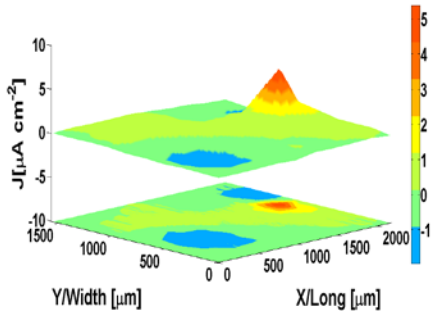

Figure 10. Current density maps for Au-Cu pair treated with 1 mM ATA in 1 mM NaCl at 6 min (a), 30 min (b) and 60 min (c).

The current density maps of Au-Cu ATA treated pair are presented in Figure 10, in a similar fashion to what was observed in the naked Au-Cu pair it is possible to resolve both metallic surfaces, with the all of the anodic activity concentrating in Cu surface and gold behaving exclusively as a cathode.

What's interesting to notice is the fact that the current density range increases when the sample has been treated with ATA. The naked sample has a maximum anodic current of 2.2 µA cm^{-2} and a maximum cathodic current of -2 µA cm^{-2} while the treated sample presents a maximum anodic current of 6.3 µA cm^{-2} and a maximum cathodic current of -2.3 µA cm^{-2}.

Since the greater change occurs in the anodic current, it is reasonable to say that ATA is facilitating the electron transfer between the metal, in this case copper, and the solution.

There is also a large non-zero region between both metals which electrochemical activity lies between 0 and 1 µA cm^{-2}, given that this zone is composed by resin, which is non-conductive, we can attribute this electrochemical activity to ionic flux in the solution.

The presence of ATA turns the OCP of the Au-Cu pair to more positive values (Table 1) compared to the one registered in 1mM NaCl, this will lead us to believe that Ata is protecting the pair. However, as we can see from the current density maps, this is not the case; on the contrary ATA increases the current density range accelerating both the anodic and cathodic processes.

3.3.2.6. Au-Cu sample treated with 2MBT

a)

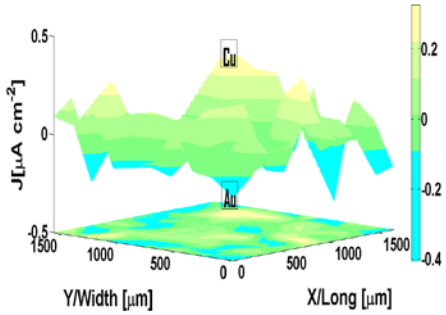

b)

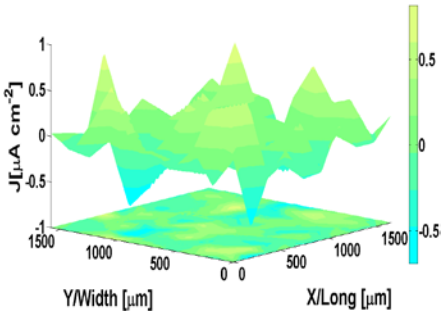

c)

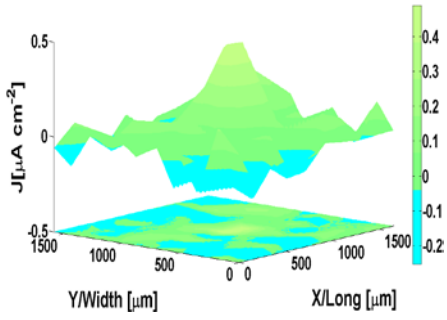

Figure 11. Current density maps for Au-Cu pair treated with 1 mM 2MBT in 1 mM NaCl at 6 min (a), 30 min (b) and 60 min (c).

Figure 11 presents the current density maps of the Au-Cu galvanic pair treated with 2MBT, as we can see the behavior of the galvanic pair is very different when is treated with 2MBT, in fact the presence of 2MBT lowers the current density range, setting the anodic maximum at 0.55 μA cm^{-2} and the cathodic maximum at -0.53 μA cm^{-2} and also makes impossible to resolve the metallic surfaces.

Initially it is possible to partially resolve Cu surface however, after 30 minutes, all electrochemical activity corresponds to ionic flux in solution, which renders the resolution of both metallic surfaces impossible.

The electrochemical activity observed in the treated Au-Cu pair is very similar to the one observed in naked Cu and Au samples, as discussed before, in the case of gold is due to the low reactivity in NaCl solution and in the case of Cu is because of the formation of a protective corrosion product layer.

However, in this case neither of both explanations is applicable, because of the electric coupling both metals are forced to act as cathode, in the case of gold, and as anode, in the case of copper. Therefore, the only possible explanation is the presence of an insulating element that is preventing the electrolyte form interacting with the metal surface, that insulating element will be the film of adsorbed 2MBT present in both metals.

It's worth noticing that Cu initially behaves like an anode but reduces is electrochemical activity to almost cero, this could be due to 2MBT molecules being desorbed and resuming their tautomeric equilibrium in a very similar fashion to what's observed in the case of 2MBT treated Au.

The presence of 2MBT makes the OCP of the Au-Cu pair more negative (Table 1) but, as has been suggested previously, this could be due to the adsorption process itself and the tautomeric equilibrium established by 2MBT in aqueous solution.

4. Conclusions

The presence of ATA and 2MBT on copper and gold samples modifies the OCP of both metals. In the case of ATA the OCP for gold is turned to a more positive value (ΔOCP=33.7 mV) than the one registered in NaCl, while copper becomes slightly more negative

(ΔOCP=-10.5 mV), 2MBT makes the OCP of gold more negative (ΔOCP=-57.7 mV), while copper becomes considerably more negative (ΔOCP=-131 mV). At the light of OCP measurements it could seem that these compounds are not good copper corrosion inhibitors since both of them turn the OCP, of the metal they are intended to protect, to more negative values.

Furthermore, the energy calculations obtained with the EQCM show that both inhibitors are physisorbed on both metals, given that the main protection mechanism attributed to organic inhibitors is the formation of physical barrier between the aggressive media and the metal, the fact that they are not chemisorbed means that their adhesion to the surface is not very strong and therefore the efficiency of the adsorbed film as a physical barrier is compromised.

However, the current density maps obtained by SVET show that, at least in the case of 2MBT, there is a significant reduction in the current density range for the Cu treated sample, for Au there is an increase in current density on the treated sample nonetheless this can be attributed to the tautomeric equilibrium of 2MBT, the galvanic pair has a similar behavior to the one observed in copper reducing considerably the current density range.

On the contrary, ATA has no effect on the gold sample presenting no variations in the current density of the system, in the case of copper it increases the current density range and facilitates the resolution of the metallic surface showing anodic and cathodic areas on the sample, a clear indication of an accelerated corrosion process, a similar behavior can be observed in the ATA treated galvanic pair, with an increased current density range and better sample resolution.

Considering the obtained results, we can conclude that although the OCP and EQCM measurements do not point to these compounds (ATA and 2MBT) as good corrosion inhibitors the SVET scans tell a different history in the case of 2MBT, showing that this compound is capable of reducing significantly the current density range of Cu and Au-Cu treated samples. However, ATA acts as an electron transfer mediator for Cu and Au-Cu

samples, increasing the current density range and facilitating the resolution of the sample's surface and acting, in this way, as corrosion catalyst rather than a corrosion inhibitor.

References

[1] ASM Specialty Handbook Copper and Copper Alloys, ASM International, 2001.

[2] N. K. Allam, A. A. Nazer, E. A. Ashour, A review of the effects of benzotriazole on the corrosion of copper and copper alloys in clean and polluted environments, J. Appl. Electrochem. 39 (2009) 961.

[3] J. A. Ramírez Cano, L. Veleva, Direct measurement of the adsorption kinetics of 2-Mercaptobenzothiazole on a microcrystalline copper surface, Rev. Metal. 52(1) (2016).

[4] D. A. Winkler, M. Breedon, A. E. Hughes, F. R. Burden, A. S. Barnard, T. G. Harvey, I. Cole, Towards chromate-free corrosion inhibitors: structure-property models for organic alternatives, Green Chem. 16 (2014) 3349.

[5] M. Finšgar, D. K. Merl, An electrochemical, long-term immersion, and XPS study of 2-mercaptobenzothiazole as a copper corrosion inhibitor in chloride solution, Corros. Sci. 83 (2014) 164.

[6] R. Subramanian, V. Lakshminarayanan, Effect of adsorption of some azoles on copper passivation in alkaline medium, Corros. Sci. 44 (2002) 535.

[7] J. C. Marconato, L. O. Bulhões, M. L. Temperini, A spectroelectrochemical study of the inhibition of the electrode process on copper by 2-mercaptobenzothiazole in etha- nolic solutions, Electrochim. Acta 43 (1998) 771.

[8] E. Cano, J.L. Polo, A. La Iglesia, J.M. Bastidas, "A study on the adsorption of benzotriazole in hydrochloric acid using the inflection point of the isotherm", Adsorption 10, 219-225 (2004).

[9] Philipe M.,Florian M., 2005. Analytical Methods in Corrosion Science and Engineering. CRC Press.

[10] R.M. Souto, Y. González-García, S. González, G.T. Burstein, Damage to paint coatings caused by electrolyte immersion as observed in situ by scanning electrochemical microscopy, Corros. Sci. 46 (2004) 2621.

[11] R.M. Souto, Y. González-García, S. González, Characterization of coating systems by scanning electrochemical microscopy: Surface topology and blistering, Prog. Org. Coat. 65 (2009) 435.
[12] Y. González-García, G.T. Burstein, S. González, R.M. Souto, Imaging metastable pits on austenitic stainless steel in situ at the open circuit corrosion potential, Electrochem. Commun. 6 (2004) 637.

[13] A.M. Simões, A.C. Bastos, M.G. Ferreira, Y. González-García, S. González, R.M. Souto, Use of SVET and SECM to study the galvanic corrosion of an iron–zinc cell, Corros. Sci. 49 (2007) 726.

[14] J. Izquierdo, J.J. Santana, S. González, R.M. Souto, Uses of scanning electrochemical microscopy for the characterization of thin inhibitor films on reactive metals: The protection of copper surfaces by benzotriazole, Electrochim. Acta 55 (2010) 8791.

[15] J.Izquierdo, J.J. Santana, S. González, R.M. Souto, Scanning microelectrochemical characterization of the anti-corrosion performance of inhibitor films formed by 2-mercaptobenzimidazole on copper, Prog. Org. Coat. 74 (2012) 526.

[16] J. Izquierdo, L. Nagy, Á. Varga, J.J. Santana, G. Nagy, R.M. Souto, Spatially resolved measurement of electrochemical activity and pH distributions in corrosion processes by scanning electrochemical microscopy using antimony microelectrode tips, Electrochim. Acta 56 (2011) 8846.

[17] J. Izquierdo, L. Nagy, J.J. Santana, G. Nagy, R.M. Souto, A novel microelectrochemical strategy for the study of corrosion inhibitors employing the scanning vibrating electrode technique and dual potentiometric/amperometric operation in scanning electrochemical microscopy: Application to the study of the cathodic inhibition by benzotriazole of the galvanic corrosion of copper coupled to iron, Electrochim. Acta 58 (2011) 707.

[18] J. Izquierdo, L. Nagy, Á. Varga, I. Bitter, G. Nagy, R.M. Souto, Scanning electrochemical microscopy for the investigation of corrosion processes: Measurement of Zn^{2+} spatial distribution with ion selective microelectrodes, Electrochim. Acta 59 (2012) 398.

[19] J. Telegdi, A. Shaban, E. Kálman, EQCM study of copper and iron corrosion inhibition in presence of organic inhibitors and biocides, Electrochim. Acta 45 (2000) 3639.

[20] C. Eickes, J. Rosenmud, S. Wasle, K. Doblhofer, K. Wang, K. G. Weil, The electrochemical quartz crystal microbalance (EQCM) in the studies of complex electrochemical reactions, ElectrochimicaActa 45 (2000) 3623.

[21] D. S. Karpovich, G. J. Blanchard, Direct measurement of the adsorption kinetics of alkanethiolate self-assembled monolayers on a microcrystalline gold surface, Langmuir 10 (1994) 3315.

[22] M. Finšgar, EQCM and XPS analysis of 1,2,4-triazole and 3-amino-1,2,4-triazole as copper corrosion inhibitors in chloride solution, Corrosion Science 77 (2013) 350.

[23] R. Répánszki, Z. Kerner, G. Nagy, “Adsorption of fission products on stainless steel and zirconium”, Adsorption 13, 201-207 (2007).

[24] El-Sayed M. Sherif, R. M. Erasmus, J. D. Comins, Effects of 3-amino-1,2,4-triazole on the inhibition of copper corrosion in acidic chloride solutions, J. Colloid Interface Sci. 311 (2007) 144.

[25] El-Sayed M. Sherif, R. M. Erasmus, J. D. Comins, Corrosion of copper in aerated synthetic sea water solutions and its inhibition by 3-amino-1,2,4-triazole, J. Colloid Interface Sci. 309 (2007) 470.

[26] Atkins P. W., 1999. Physical Chemistry. Oxford University Press, 857-858.

[27] J. A. Ramírez Cano, L. Veleva, Adsorption kinetics of benzothiazole and 2-mercaptobenzothiazole on microcrystalline gold and silver surfaces, Solid State Phenom. 227 (2015) 99.

[28] M. H. Palmer, D. Christen, An ab initio study of the structure, tautomerism and molecular properties of the C- and N-amino-1,2,4-triazoles, J. Mol. Struct. 705 (2004) 177.

[29] K. Sayin, H. Jafari, F. mohsenifar, Effect of pyridil on adsorption behavior and corrosion inhibition of aminotriazole, J. Taiwan Inst. Chem. Eng. 68 (2016) 431.

[30] F. Altaf, R. Qureshi, S. Ahmed, Surface protection of copper by azoles in borate buffers-voltametric and impedance analysis, J. Electroanal. Chem. 659 (2011) 134.

[31] M. M. Antonijević, S. M. Milić, M. B. Petrović, Films formedon copper Surface in chloride media in the presence of azoles,Corros. Sci. 51 (2009) 1228.

[32] J. C. Puerta, V. Del Campo, R. Henríquez, P. Häberle, Resistivity of thiol-modified gold thin films, Thin Solid Films 570 (2014) 150.

[33] A. Pallipurath, O. Nicoletti, J. M. Skelton, S. Mahajan, P. A. Midgley, S. R. Elliot, Surfactant-free coating of thiols on gold nanoparticles using sonochemistry: A study of competing processes, UltrasonicsSonochemistry 21 (2014) 1886.

[34] M. Frasconi, F. Mazzei, T. Ferri, Protein immobilization at gold-thiol surfaces and potential for biosensing, Anal.Bioanal. Chem. 398 (2010) 1545.

[35] M. Ohsawa, W. Suëtaka, Spectro-electrochemical studies of the corrosion inhibition of copper by mercaptobenzothiazole, Corros. Sci. 19 (1979) 709.